A BAG3 Coding Variant in Mice Determines Susceptibility to Ischemic Limb Muscle Myopathy by Directing Autophagy

Joseph M. McClung, Timothy J. McCord, Terence E. Ryan, Cameron A. Schmidt, Thomas D. Green, Kevin W. Southerland, Jessica L. Reinardy, Sarah B. Mueller, Talaignair N. Venkatraman, Christopher D. Lascola, Sehoon Keum, Douglas A. Marchuk, Espen E. Spangenburg, Ayotunde O. Dokun, Brian H. Annex and Christopher D. Kontos

Circulation. published online April 25, 2017;
Circulation is published by the American Heart Association, 7272 Greenville Avenue, Dallas, TX 75231

Print ISSN: 0009-7322. Online ISSN: 1524-4539

A BAG3 Coding Variant in Mice Determines Susceptibility to Ischemic Limb Muscle Myopathy by Directing Autophagy

SUPPLEMENTAL MATERIAL

Short Title: McClung, BAG3 variation determines ischemia susceptibility

Joseph M. McClung[1,2]# PhD, Timothy J. McCord[3] BS, Terence E. Ryan[1,2] PhD, Cameron A. Schmidt[1,2] BS, Tom D. Green[1,2] BS, Kevin W. Southerland[4] MD, Jessica L. Reinardy[3,5] PhD, Sarah B. Mueller[3,5] PhD, Talaignair N. Venkatraman[6] PhD, Christopher D. Lascola[6] MD, Sehoon Keum[7] PhD, Douglas A. Marchuk[7] PhD, Espen E. Spangenburg[1,2] PhD, Ayotunde Dokun[8,10] MD, Brian H. Annex[8,9,10] MD, Christopher D. Kontos[3,5] MD

[1]Department of Physiology, [2]Diabetes and Obesity Institute, East Carolina University, Brody School of Medicine, Greenville, NC. [3]Department of Medicine, Division of Cardiology; [4]Department of Surgery, Division of General Surgery; [5]Department of Pharmacology and Cancer Biology; [6]Department of Radiology; [7]Department of Molecular Genetics and Microbiology; Duke University Medical Center, Durham, NC. [8]Department of Medicine, Division of Endocrinology; [9]Division of Cardiovascular Medicine; [10]The Robert M. Berne Cardiovascular Research Center; University of Virginia School of Medicine, Charlottesville, VA

#Correspondence should be addressed to J.M.M.: 4109 East Carolina Heart Institute, Mail Stop 743. 115 Heart Drive, Greenville, NC 27834; Tel: 252-737-5034; Fax: 252-744-0462; email: mcclungj@ecu.edu.

Detailed Materials and Methods

Animals. Experiments were conducted on adult C57BL/6 (BL6; *N*=34), BALB/c (*N*=151), or BALB/c congenic mice (Congenic, C.B6-*Lsq1-3* or also known as C.B6-*Civq1-3*[1]; *N*=5) (≥ 10 weeks old), approved by either the East Carolina University, Duke University, or University of Virginia Animal Care and Use Committees and conformed to the Guide for the Care and Use of Laboratory Animals published by the US National Institutes of Health. Briefly, hindlimb ischemia[2] was performed by anesthetizing mice by intraperitoneal injection of ketamine (90 mg/kg) and xylazine (10 mg/kg) and surgically inducing unilateral hindlimb ischemia with ligation and excision of the femoral artery from its origin just above the inguinal ligament to its bifurcation at the origin of the saphenous and popliteal arteries. The inferior epigastric, lateral circumflex, and superficial epigastric artery branches were also isolated and ligated. After induction of ischemia semiquantitative necrosis scoring and laser Doppler perfusion monitoring were performed as described below. Ischemia surgeries and necrosis scoring on virus-treated animals were performed in several cohorts of animals from 3 laboratories at 3 institutions by blinded investigators for effect validation. A subset of BL6 and BALB/c animals were subjected to a modified version of hindlimb ischemia as previously described[3], where the femoral artery was singularly ligated and transected just inferior to the inguinal ligament and the inferior epigastric, lateral circumflex, and superficial epigastric artery collateral branches were left intact. The cardiotoxin (CTX) model of mouse muscle regeneration was performed as previously described[4] using 20 μL I.M. injections of 5 μM *Naja nigricollis* venom into the tibialis anterior (TA) muscle under anesthesia. An equivalent volume sham injection of 1× phosphate buffered saline (PBS) was administered to the muscles of the contralateral hindlimb. The full breakdown of animal usage per experimental group (across all Institutions) is as follows: 1) parental BL6 mice for HLI (*N*=24); 2) BL6+AAV-BAG3^{Met81} for HLI (*N*=5); 3) Congenic mice for HLI (*N*=5); 4)

BALB/c mice for HLI (*N*=15); 5) BALB/c+AAV-GFP for HLI (*N*=30); 6) BALB/c+AAV-BAG3^{Met81} for HLI (*N*=21); BALB/c+AAV-BAG3^{Ile81} for HLI (*N*=22); 7) BALB/c+AAV-GFP for CTX (*N*=4); 8) BALB/c+AAV-BAG3^{Met81} for CTX (*N*=4); 9) BALB/c+AAV-BAG3^{Ile81} for CTX (*N*=4); 10) BL6 for modified HLI (*N*=5); 11) BALB/c+AAV-GFP for modified HLI (*N*=5); 12) BALB/c+AAV-BAG3^{Met81} for modified HLI (*N*=12); 13) BALB/c+AAV-BAG3^{Ile81} for modified HLI (*N*=10); 14) BALB/c for cell isolations (*N*=24).

Assessment of tissue necrosis. The extent of necrosis, if any, in ischemic limbs was recorded post-operatively using the previously described semi-quantitative scale [2, 5]: grade 0, no necrosis in ischemic limb; grade I, necrosis limited to toes; grade II, necrosis extending to dorsum pedis; grade III, necrosis extending to crus; and grade IV, necrosis extending to mid-tibia or complete limb necrosis. For limb necrosis, each animal was scored by a blinded investigator at each time point and all scores were assigned across each model by the same-blinded investigator.

Laser Doppler perfusion imaging. Limb blood flow was measured using laser Doppler perfusion imaging (LDPI) as previously described[3] with the following modifications. Imaging was performed at a 4ms/pixel scan rate on animals placed on a 37°C warming pad in the prone position under ketamine/xylazine anesthesia using a Moor Instruments LDI2-High Resolution (830 nM) System (Moor, Axmin- ster, UK). Hindlimb hair was removed with depilatory cream 24 hours prior to initial scanning and hair was removed with a microshaver at all other timepoints. Images were analyzed with the MoorLDI Image Review software. Mice were closely monitored during the postoperative period and flow in the ischemic and contralateral non-ischemic limbs was measured immediately after surgery to verify successful surgery.

Magnetic resonance (MR) imaging. MR imaging was performed on a Bruker 7T (70/30) system (Bruker Biospin, Billerica, MA, USA) utilizing a quadrature surface receive and volume transmit coil set-up with active decoupling. Animals were anesthetized (induction: 5% isoflurane, maintenance 1.5% isoflurane, with room air mixture) and placed in an MRI-compatible cradle

equipped to maintain body temperature constant using warm water circulation. Temperature and respiratory rate were continuously monitored. T2-weighted anatomic images were first acquired using a RARE-based fast spin echo sequence with TR=4200, TE=12, RARE factor 8, 1 mm slice thickness, FOV 2.4 cm, 256 x 256, with respiratory gating. T2 images are displayed as 3D maximum intensity projection images for correlation to MR angiography (MRA). MRA was performed using a contrast-enhanced T1-weighted time-of-flight sequence in the coronal plane with 2D FLASH, using TE/TR + 3.8/15 ms, FOV = 4 cm x 4 cm, matrix of 256 x 256, and 120 slices. Vascular contrast was enhanced utilizing intravenous gadofosveset trisodium (ABLAVAR, Lantheus Medical Imaging, Inc.), at 0.03 mmol/Kg. This agent is clinically approved for optimization of blood pool imaging by virtue of specific binding to serum albumin. Perfusion maps were then generated using a double spin-echo planar pulse sequence using pairs of bipolar gradients at specific predetermined signs in each of three orthogonal directions. The combination of gradient directions allows cancellation of all off-diagonal tensor elements, enabling measurement of the diffusion tensor trace, and therefore providing unambiguous and rotationally invariant ADC values. Four *b* values (*b* = 0, 50.0, 100, and 200) were acquired, with a matrix size of 128 x 128, slice thickness 1.0 mm. Volume images (one for each *b* value) were created from raw DICOM images. For voxels within the 128×128×15 matrix with a signal value above 2000, the apparent diffusion coefficient (ADC) at each voxel was calculated using an exponential moving fit by the following method: ADC = ln [S(b=b_1) – S(b=b_2)/b_2-b_1. *B*1 and *b*2 values of 100 and 200, respectively, are sensitive to blood flow apparent diffusion changes in small arteries and capillaries. ADC maps were generated using mono-exponential fitting as above, and T2 images were zero-filled to 256×256 prior to analysis. Parametric images were analyzed in anatomic regions of interest (ROIs) using Bruker Paravision software and offline using Osirix software.

Muscle contractile force measurements. Contractile force measurements were performed using extensor digitorum longus (EDL) muscles as previously described[6]. In brief, single EDL muscles were surgically excised with ligatures at each tendon (5–O silk suture) and mounted in a bath between a fixed post and a force transducer (Aurora 300B-LR) operated in isometric mode. The muscle was maintained in modified Krebs buffer solution (PSS; pH 7.2) containing 115 mM NaCl, 2.5 mM KCl, 1.8 mM $CaCl_2$, 2.15 mM Na_2HPO_4, and 0.85 mM NaH_2PO_4, and maintained at 25°C under aeration with 95% O_2–5% CO_2 throughout the experiment. Resting tension and muscle length were iteratively adjusted for each muscle to obtain the optimal twitch force, and a supramaximal stimulation current of 600mA was used for stimulation. After a 5 min equilibration, isometric tension was evaluated by 200 ms trains of pulses delivered at 10, 20, 40, 60, 80, 100, and 120 Hz. Length was determined with a digital microcaliper. After the experimental protocol, muscles were trimmed proximal to the suture connections, excess moisture was removed, and the muscle was weighed. The cross-sectional area for each muscle was determined by dividing the mass of the muscle (g) by the product of its length (L_0, mm) and the density of muscle (1.06 g/cm^3) and was expressed as millimeters squared (mm^2). Muscle output was then expressed as specific force (N/cm^2) determined by dividing the tension (N) by the muscle cross-sectional area[7].

RNA Isolation and RT-PCR. Total RNA was extracted using Trizol-phenol/chloroform isolation procedures and was reverse-transcribed using Superscript III Reverse Transcriptase and random primers (Invitrogen Inc.). Real-time PCR was performed using a 7500 Real-Time PCR System (Applied Biosystems, Foster City, CA). Relative quantification of *Bag3* mRNA levels was determined using the comparative threshold cycle ($\Delta\Delta$CT) method using FAM TaqMan® Gene Expression Assays (Applied Biosystems) specific to the given gene run in complex (multiplex) with a VIC-labeled GAPDH control primer.

123 *Primary Antibodies and Materials.* The following commercial antibodies were used: FLAG,
124 LC3b, ATG7, Beclin, HspB8, SQSTM1/p62 (Cell Signaling), BAG3 (Polyclonal, Imgenex),
125 GAPDH (Novus Biologicals), tubulin (Santa Cruz), CD31 (Abd Serotec MCA-1364), SMA
126 (DAKO, 1A4). For immunofluorescence: Dystrophin (Thermo Scientific RB-9024), and Pax7,
127 eMyHC (F1.652), and Dystrophin (MANDYS1 3B7) (all from Developmental Studies Hybridoma
128 Bank, Iowa City, IA), CD31 (Abd Serotec MCA-1364), and SMA (DAKO, 1A4). The TSA
129 amplification kit (#24, with HRP-streptavidin and Alexa Fluor 568 tyramide, Molecular Probes)
130 was utilized exclusively for Pax7 immunofluorescence.
131 *Histological analysis.* Skeletal muscle morphology, vessel density, and markers of muscle
132 regeneration were assessed by standard light microscopy and immunofluorescence microscopy
133 as previously described[3]. Eight-μm-thick transverse sections were cut from mouse TA muscle,
134 frozen in liquid nitrogen-cooled isopentane in optimum cutting temperature (OCT) medium.
135 Sections were allowed to come to room temperature and were either stained with hematoxylin
136 and eosin using standard methods or fixed and permeabilized with ice-cold acetone for 10 min
137 at 4°C. Sections from TA muscle samples were stained with H&E, and digital images were
138 obtained at ×10 magnification for the analysis of non-contractile tissue expansion. A 528
139 (22X24)-point grid was overlain on 3 images from each animal, and points were analyzed for
140 occurrence on myofibers or outside of myofibers and expressed as the percentage of non-
141 myofiber area in HLI muscle as an indication of muscle myofiber reformation and hypertrophy.
142 For the analysis of myofiber integrity, approximately 300 individual fibers visualized by
143 immunofluorescence labeling for dystrophin and DAPI were quantified for disrupted dystrophin
144 staining (>50% of fiber membrane area dystrophin negative) and expressed as the percentage
145 of total fibers with intact dystrophin immunostaining (% intact TA myofibers). Total or eMyHC+
146 myofiber cross sectional area (CSA, μm^2) was determined using ×10 images by analyzing

147 approximately 300 individual fibers with NIH ImageJ image analysis software. Images were
148 also utilized for the localization of centralized myofiber nuclei, expressed as a percentage of
149 total myofibers with centralized nuclei.
150 *Immunofluorescence (IF).* IF was used for the visualization of muscle morphology, vessel
151 density, and muscle regeneration. 8-μm-thick transverse sections were cut from TA muscle
152 frozen in liquid nitrogen cooled isopentane in OCT. Sections were allowed to come to room
153 temperature and fixed/permeabilized with ice-cold acetone for 10 min at 4°C. Fixed sections
154 were rehydrated in 1× PBS before blocking in 5% normal goat serum (Sigma) in 1× PBS at RT
155 for 45 min. Slides were then incubated overnight at 4°C in a primary antibody solution. Slides
156 were then washed 3× in 1× PBS at RT and incubated for 1h at RT in the dark in a secondary
157 solution containing a 1:250 dilution of Alexa Fluor 488-, 568-, or 633-conjugated secondary
158 antibodies in blocking solution. Sections were then washed in the dark 3× for 5 min each with 1×
159 PBS at RT, and slipcovers were mounted using Vectashield HardSet Mounting Medium with
160 DAPI (Vector Labs H-1500). Images were captured using a Zeiss Axio Observer Inverted Laser
161 Scanning Microscope (LSM) 510 utilizing the Zeiss LSM 510 software (v. 4.2) and analyzed by a
162 blinded investigator using ImageJ software (NIH, v. 1.49v). Vessel density was quantified as the
163 number of $CD31^+$ cells per μm^2 of muscle analyzed. The density of $CD31^+$ vessels was
164 quantified as an indicator of capillary density changes in the distal limb muscle and represents
165 capillary regression or angiogenesis. Pax7 staining was performed as previously described [8].
166 Sections were then washed 3× for 5 min in the dark with 1×PBS at RT and slipcovers were
167 mounted using Vectashield HardSet Mounting Medium with DAPI (Vector Labs H-1500). Images
168 were captured using a Zeiss Axio Observer Inverted Laser Scanning Microscope (LSM) 510
169 utilizing the Zeiss LSM 510 version 4.2 software and analyzed using NIH ImageJ software as
170 follows: CD31+, SMA+, PAX7+, and eMyHC+ labeled cells were counted and expressed as the

ratio of positively stained cells/ μ m^2 of TA muscle analyzed. Representative immunofluorescence images from animals infected with AAV-GFP viruses were pseudo-colored green for visualization.

SDS-PAGE, western blotting (WB), and immunoprecipitation (IP). SDS-PAGE and WB were performed according to standard methods. Frozen muscles were homogenized in ice-cold RIPA lysis buffer containing protease and phosphatase inhibitors. Protein concentrations were determined using a BCA protein assay (Pierce, ThermoFisher #23225). Proteins were then separated by SDS-PAGE (Mini-Protean TGX, Bio-Rad #4561093) with equal amounts of total protein loaded per well. For IP, total protein lysates from limb tissues or cell lysates were generated in lysis buffer supplemented with protease and phosphatase inhibitor tablets (Complete PI, PhosSTOP, Roche USA) and allowed to rotate with monoclonal Anti-FLAG Affinity Gel (Sigma, A2220) or BAG3 primary antibody o/n at 4°C. Immunoprecipitation experiments were performed 3 independent times.

Cell Lines and Culture. Murine C2C12 and C3H-10T1/2 cell lines were purchased from ATCC and cultured as per the manufacturer's recommendations. Differentiation was stimulated by serum withdrawal in differentiation medium (DM: DMEM supplemented with 2% horse serum, 1% penicillin/streptomycin, 0.2% amphotericin B, and 0.01% human insulin/transferrin/selenium). To evaluate the effects of ischemia/hypoxia in skeletal muscle cells *in vitro*, we have established a model of cellular hypoxia in which cells are subjected to 0% O_2 and deprived of nutrients in Hanks' balanced salt solution (HBSS) [9] to mimic the local environment resulting from severe ischemia in PAD (referred to hereafter as hypoxia+nutrient deprivation, HND). GP2-293 cells for pantrophic retrovirus generation were cultured at 37°C and 5% CO2 in DMEM with 10% FBS. Transfections were done with Lipofectamine-Plus reagent (Invitrogen).

Primary Myoblast Isolation and Culture. Primary murine muscle precursor cells (mouse myoblasts) derived from hindlimb muscles were prepared as previously described [5]. Briefly, peripheral skeletal muscle was dissected from 6-week old female mice using sterile technique, trimmed of connective tissue, and placed in 10-cm dishes containing ice cold sterile PBS. Organs were then transferred to separate 10-cm dishes containing 5mL of pre-warmed MPC isolation medium (IM: DMEM with 4.5g/L glucose, supplemented with 1% Penicillin/Streptomycin/Amphotericin B) and any remaining connective tissue was trimmed. Organs were then transferred to a third 10-cm dish containing 5mL of cold MPC IM, transported to the sterile culture hood, and minced for 2 minutes (per plate) using sterile razor blades. The minced slurry was transferred to 15mL tubes, 5mL additional MPC IM was added, tubes were inverted several times and centrifuged at 4°C for 3min at 700 ×*g* to remove contaminants. The MPC IM was subsequently aspirated and the pellet was resuspended in 10mL of MPC IM and inverted 5-10× to loosen the pellet and mix before decanting into a 10-cm culture dish. Tubes were subsequently rinsed with 8mL MPC IM to ensure all tissue was removed, and 2mL of 1% pronase (Calbiochem #53702) was added to a final concentration of 0.1%. A sterile, low-profile magnetic stir bar was added, and dishes were stirred at low rpm on a magnetic stir plate at 37°C and 5% CO2 for 1hr. The digested tissue slurry was then transferred to 50mL conical tubes and centrifuged for 4min at 800 ×*g* at RT. The supernatant was aspirated and the digested pellet was resuspended in 10mL MPC purification medium (PM: DMEM with 4.5g/L glucose, supplemented with 10% fetal bovine serum and 1% Penicillin/Streptomycin/Amphotericin B). The suspension was then triturated approximately 20× through a blunt end pipetting needle attached to a sterile 30cc syringe. The suspension was then passed through a 100 μm disposable Steriflip vacuum filter into a 50mL tube, including 3 successive 8mL washes of the sieve with pre-warmed PM, and subsequently centrifuged at RT 5min at 1000 ×*g*. The cell pellet

was then resuspended in 1mL FBS before addition to primary MPC growth medium (GM: Ham's F10, supplemented with 20% FBS and 1% Penicillin/Streptomycin/Amphotericin B, and supplemented immediately prior to use with 5ng/mL basic FGF). Cells were plated on collagen-coated T150 flasks, allowed to adhere and proliferate for 3-days, and subsequently trypsinized with 0.25% Trypsin/EDTA and pre-plated at 37°C and 5% CO2 for 1hr on an uncoated T150 flask to allow for fibroblast removal. The supernatant containing the MPCs was removed and centrifuged at 800 ×*g* for 5min at RT prior to re-plating in MPC GM on collagen-coated T150 flasks. After reaching approximately 70% confluence, MPCs were then plated in pre-warmed GM in either T75 flasks or standard 12-well culture plates coated with entactin/collagen/laminin and allowed to reach approximately 90% confluence. Confluent MPCs were then rinsed once in sterile PBS and switched to DM for myotube formation. DM was changed every 24 hours. Cell purity of myoblasts was verified by immunofluorescence staining for MyoD and DAPI followed by counting the number of MyoD-stained cells as a percentage of total nuclei. Purity of myotubes was also analyzed by immunofluorescence staining of myosin heavy chain (MyHC) and DAPI after differentiation into myotubes.

Proliferation, apoptosis, and myotube fusion index assays. Muscle myoblast cell proliferation was assessed by plating approximately 50,000 strain-specific and/or pre-infected (GFP, $BAG3^{Met81}$, or $BAG3^{Ile81}$ AAVs: 1×10^9 AVP) cells on 6-well plates coated with entactin/collagen/laminin (ECL). Wells were washed with phosphate-buffered saline (PBS), fixed with 100% methanol for 5 min, and left to air dry for 10 min. All experimental wells were then simultaneously stained with hematoxylin for 5-minutes and rinsed 3× in dH_20. Cell images were obtained via phase contrast at ×10 magnification on an inverted microscope camera system. Total image cell counts were quantified from at least 4 random fields, a number chosen by determination of no additional change in standard deviation, by a blinded investigator. Muscle

proliferation numbers were then normalized by treatment to the 0-hour (post-plating) counts to give fold population doubling values. Cellular apoptosis/necrosis was quantified using ApoAlert Annexin V kit (Clontech). Cells were stained with Annexin V-FITC, propidium iodide and DAPI and assessed under standard fluorescent microscopy. Immunofluorescence for myosin heavy chain (MyHC) and nuclei (DAPI) was performed for myotube fusion analysis as previously described[10]. Approximately 100,000 cells per treatment/strain were plated on 12-well plates coated with ECL, allowed to reach 50-60% confluence in primary GM, and infected with either control (GFP), BAG3^{Met81}, or BAG3^{Ile81} AAVs (2×10^9 AVP) for 24hrs in DM. DM was then changed every 24hours. Cells were washed with phosphate-buffered saline (PBS), fixed with 100% methanol for 5 min, left to air dry for 10 min, and immunofluorescently labeled with anti-MyHC. Images were captured using a Life Technologies EVOS auto FL wide field fluorescence microscope (Thermo Fisher) and analyzed by a blinded investigator using ImageJ (NIH, v1.49). Each well was photographed in four randomly selected regions. The number of myonuclei and the total number of nuclei were scored and the fusion index was calculated as the percentage of total nuclei incorporated in myotubes. Each experiment included at least 3 technical replicates and each biological experiment was replicated at least 3 times.

Virus Generation. Pantrophic BAG3 shRNA or GFP control retroviruses were generated by cotransfection of GP2-293 cells with shRNA plasmids (SABiosciences) and envelope plasmid (VSVG). BAG3 shRNA (sequence derived from TRCN0000293298, Sigma-Aldrich) or scrambled (scr) Control (Sigma-Aldrich) annealed oligos were also ligated into pLKO.1-TRC cloning vector (Addgene, plasmid #10878). The full pLKO.1 shRNA cassette was cloned via In-Fusion (Clontech) into pAdeno-X PRLS Universal System 3 vector (Clontech). The insert, mRFP:EGFP:LC3 from plasmid ptfLC3 (Addgene #21074), was cloned via In-Fusion (Clontech) into the Adeno-X adenoviral vector (Clontech). Adenoviruses were generated by transfection of Adeno-X 293 cells using CalPhos Mammalian Transfection Kit (Clontech). pCMV5 containing

C-terminal FLAG-tagged coding regions of either BALB/c (Met81) or BL6 (Ile81)-specific mouse *Bag3* were moved into pTR-transgene AAV vectors in combination with XX680 for virus generation. Adeno-associated viruses (GFP, $BAG3^{Met81}$, $BAG3^{Ile81}$) were generated using mouse strain-specific constructs in suspension HEK293 cells and purified by column chromatography at the UNC Viral Vector Core Facility. AAV viruses were injected *in vivo* either 1) IM into the TA and medial and lateral gastrocnemius hindlimb muscles (1×10^{10} AVP/injection site) and allowed to express for 7 days prior to HLI; or 2) systemically (retro-orbitally; 1×10^{11} AVP/ injection) and allowed to express for 21 days prior to HLI, or they were used *in vitro* (1×10^{9} AVP). All intramuscular or systemic (retro-orbital) virus-injected animals (regardless of heterogeneity or lack of expression) were included for analysis.

Autophagic Flux. Autophagic flux was assessed in myoblasts and myotubes using an adenovirus expressing the RFP-GFP-LC3 reporter[31]. Sub-confluent myoblasts in a 12-well plate were infected with RFP-GFP-LC3 and BAG3 viruses for 8 hours in low serum medium and subjected to control or experimental ischemia conditions approximately 48-hours later. Confluent primary BALB/c myoblasts in a 12-well plate were also infected with RFP-GFP-LC3 and BAG3 viruses overnight at the time of transition to low serum differentiation medium and then allowed to differentiate for 120hrs. Images were captured using a Life Technologies Evos auto FL wide field fluorescence microscope (Thermo Fisher) and analyzed by a blinded investigator. Punctate structures with GFP-RFP and/or RFP signals were quantified in more than 120 cells per group, and the degree of autophagosome maturation was expressed as the percent of puncta with red color, as previously described[32].

Statistical Analysis. Statistical analyses were carried out using StatPlus:mac (v. 2009) statistical analysis software, Vassarstats (www.vassarstats.net), or Prism 6 (v. 6.0d). Non-parametric necrosis score and peak specific force (% Control) data were compared using Kruskal-Wallis

292 tests and Mann-Whitney U Tests, where appropriate, for post-hoc analyses. For MR
293 angiography analyses, data were evaluated using Student's *t*-test. Correlation data for BAG3
294 protein and muscle force production were performed using least squares regression procedure.
295 Data corrected for control limbs were analyzed using paired t-tests. All other data were
296 compared using ANOVA or repeated measures ANOVA with Tukey's post hoc tests or Student's
297 2-tailed *t*-test. In all cases, $P < 0.05$ was considered statistically significant and values are
298 presented as means ± SE.
299
300

Supplemental References

1. Keum S, Lee HK, Chu PL, Kan MJ, Huang MN, Gallione CJ, Gunn MD, Lo DC and Marchuk DA. Natural genetic variation of integrin alpha L (Itgal) modulates ischemic brain injury in stroke. *PLoS Genet*. 2013;9:e1003807.
2. Dokun AO, Keum S, Hazarika S, Li Y, Lamonte GM, Wheeler F, Marchuk DA and Annex BH. A quantitative trait locus (LSq-1) on mouse chromosome 7 is linked to the absence of tissue loss after surgical hindlimb ischemia. *Circulation*. 2008;117:1207-15.
3. McClung JM, McCord TJ, Southerland K, Schmidt CA, Padgett ME, Ryan TE and Kontos CD. Subacute limb ischemia induces skeletal muscle injury in genetically susceptible mice independent of vascular density. *J Vasc Surg. 2016;64(4):1101-1111.e2.*
4. Yan Z, Choi S, Liu X, Zhang M, Schageman JJ, Lee SY, Hart R, Lin L, Thurmond FA and Williams RS. Highly coordinated gene regulation in mouse skeletal muscle regeneration. *J Biol Chem*. 2003;278:8826-36.
5. McClung JM, McCord TJ, Keum S, Johnson S, Annex BH, Marchuk DA and Kontos CD. Skeletal muscle-specific genetic determinants contribute to the differential strain-dependent effects of hindlimb ischemia in mice. *The American journal of pathology*. 2012;180:2156-69.
6. Spangenburg EE, Le Roith D, Ward CW and Bodine SC. A functional insulin-like growth factor receptor is not necessary for load-induced skeletal muscle hypertrophy. *J Physiol*. 2008;586:283-91.
7. Brooks SV and Faulkner JA. Contractile properties of skeletal muscles from young, adult and aged mice. *J Physiol*. 1988;404:71-82.
8. McCarthy JJ, Mula J, Miyazaki M, Erfani R, Garrison K, Farooqui AB, Srikuea R, Lawson BA, Grimes B, Keller C, Van Zant G, Campbell KS, Esser KA, Dupont-Versteegden EE and Peterson CA. Effective fiber hypertrophy in satellite cell-depleted skeletal muscle. *Development*. 2011;138:3657-66.
9. Arany Z, Foo SY, Ma Y, Ruas JL, Bommi-Reddy A, Girnun G, Cooper M, Laznik D, Chinsomboon J, Rangwala SM, Baek KH, Rosenzweig A and Spiegelman BM. HIF-independent regulation of VEGF and angiogenesis by the transcriptional coactivator PGC-1alpha. *Nature*. 2008;451:1008-12.
10. McClung JM, Reinardy JL, Mueller SB, McCord TJ, Kontos CD, Brown DA, Hussain SN, Schmidt CA, Ryan TE and Green TD. Muscle cell derived angiopoietin-1 contributes to both myogenesis and angiogenesis in the ischemic environment. *Frontiers in physiology*. 2015;6:161.

Supplemental Figure 1

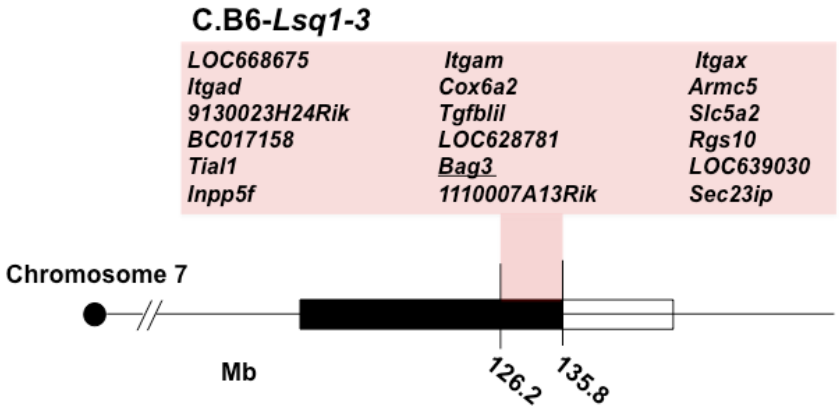

Congenic mice narrowing *Lsq-1*. BALB/c-Chr7-C57BL/6J chromosome substitution congenic strain (Congenic, C.B6-*Lsq1-3*) was generated in which a 12 MB region of Chr 7 (containing *Bag3*, among other *Lsq-1* genes), was introgressed from BL6 into the BALB/c background.

Supplemental Figure 2

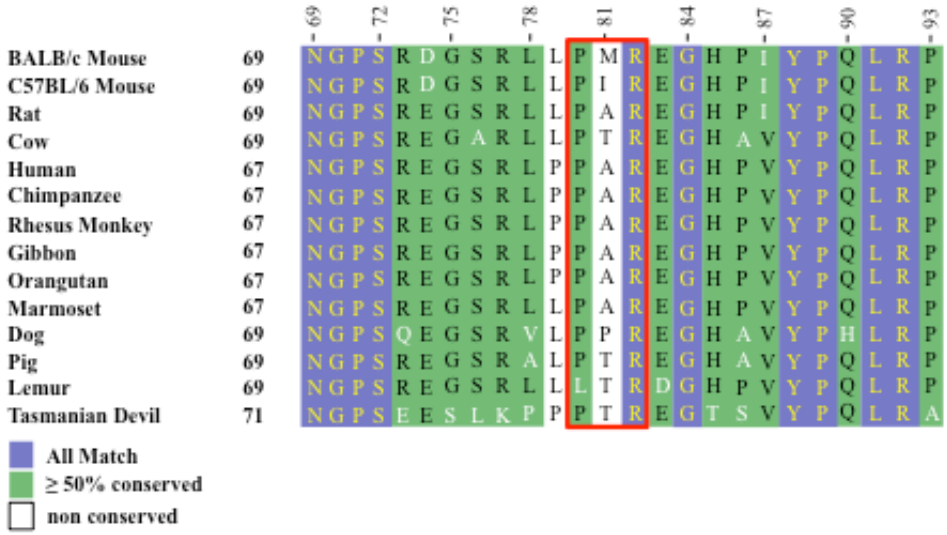

SFigure 2. BAG3 protein variation around amino acid residue 81. Alignment of BAG3 protein sequences from various species reveals a lack of conservation at amino acid residue 81 but a high degree of conservation among surrounding residues.

Supplemental Figure 3

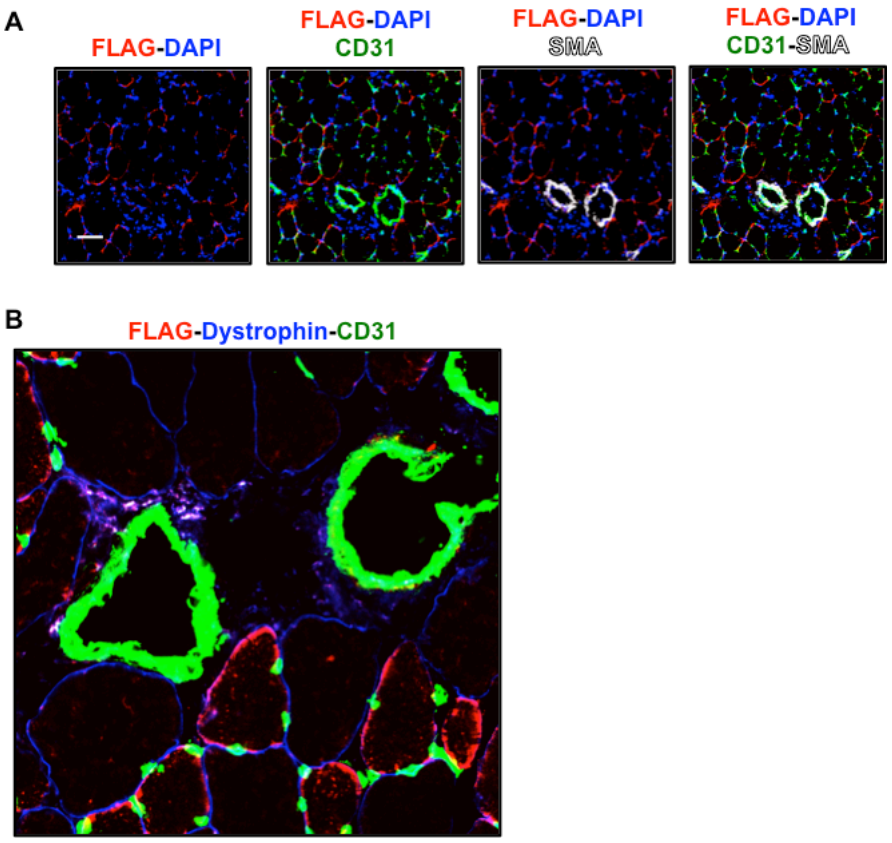

SFigure 3. Localization of AAV6-expressed FLAG-tagged BAG3. To verify the efficiency of expression of AAV6-BAG3, 2×10^{10} active viral particles (AVP) were injected into the TA muscle of non-ischemic mice. **A,B**. Muscle sections (8 μm) were immunofluorescently stained with anti-FLAG (red) and anti-CD31 (green) and co-labeled with antibodies against smooth muscle actin (SMA, white, A) or dystrophin (blue, B), and co-labeled with DAPI to stain nuclei (A) to verify efficiency of muscle tissue transgene expression.

Supplemental Figure 4

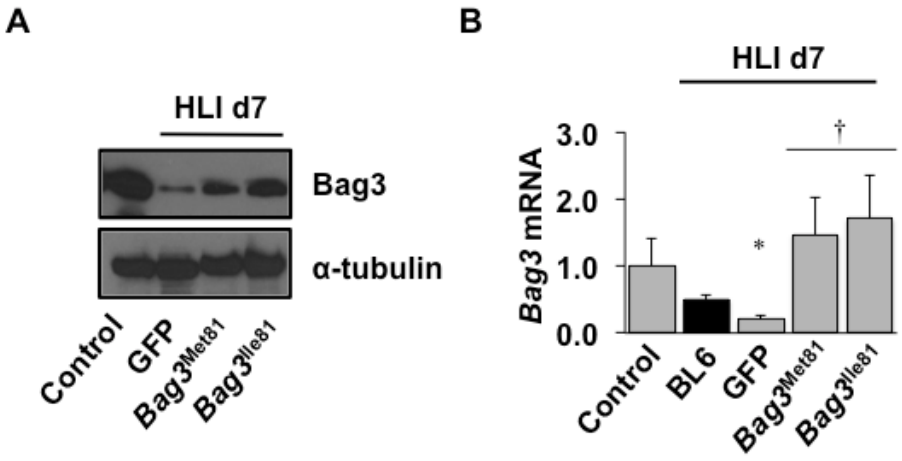

SFigure 4. Verification of BAG3 expression in ischemic limb muscle. BL6 and BALB/c mice were infected with serotype 6 adeno-associated viruses encoding GFP, $BAG3^{Met81}$, or $BAG3^{Ile81}$. Seven days later, mice were subjected to HLI, and another 7 days later tissue was harvested for analysis of BAG3 mRNA and protein expression. **A**. BALB/c skeletal muscle homogenates were western blotted for BAG3 protein expression and α-tubulin as a loading control, and non-ischemic muscle was used as a Control. **B**. Muscle from control, non-ischemic hind limb or from ischemic BL6 mice (black bar) or ischemic BALB/c mice injected with AAVs encoding the indicated proteins (gray bars) was used for qRT-PCR analysis. *P<0.05 vs. non-ischemic control (Control); †P<0.05 vs. GFP.

Supplemental Figure 5

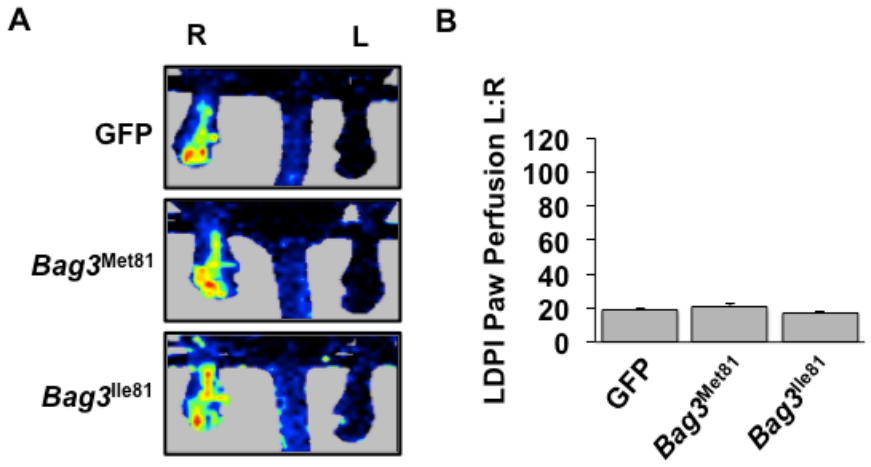

SFigure 5. AAV-infected mice display similar perfusion deficits immediately post ischemia surgery. BALB/c were infected with adeno-associated viruses encoding GFP, BAG3^{Met81}, or BAG3^{Ile81} and 7 days later were subjected to HLI. Limb blood flow was analyzed by LDPI immediately post-surgery (**A**) and quantified as a percentage of perfusion in the non-injected limb (**B**).

Supplemental Figure 6

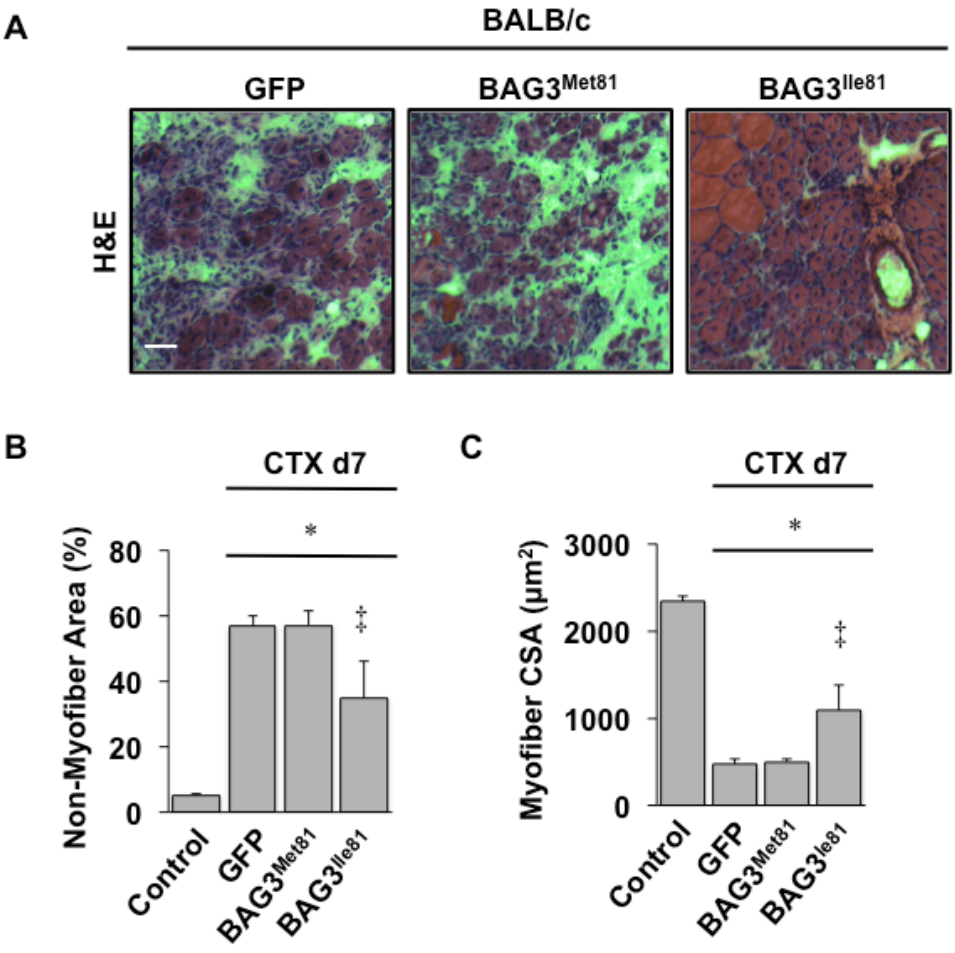

SFigure 6. BAG3^{Ile81} enhances non-ischemic muscle regeneration. Cardiotoxin (CTX, *Naja nigricolis* toxin) injection, a traditional muscle regeneration model, was performed in BALB/c mice injected IM with AAVs encoding GFP, BAG3^{Met81}, or BAG3^{Ile81} (N≥5 mice/group). The TA muscle was visualized histologically after H&E staining (**A**, scale bar = 100 μm), and non-myofiber tissue area (**B**) and myofiber cross sectional area (**C**) were quantified. Note the preservation of myofiber fascicular architecture and size with BAG3^{Ile81} expression. *P<0.05 vs. Control. ‡ P<0.05 vs. GFP or BAG3^{Met81}. All data are means ± SEM.

Supplemental Figure 7

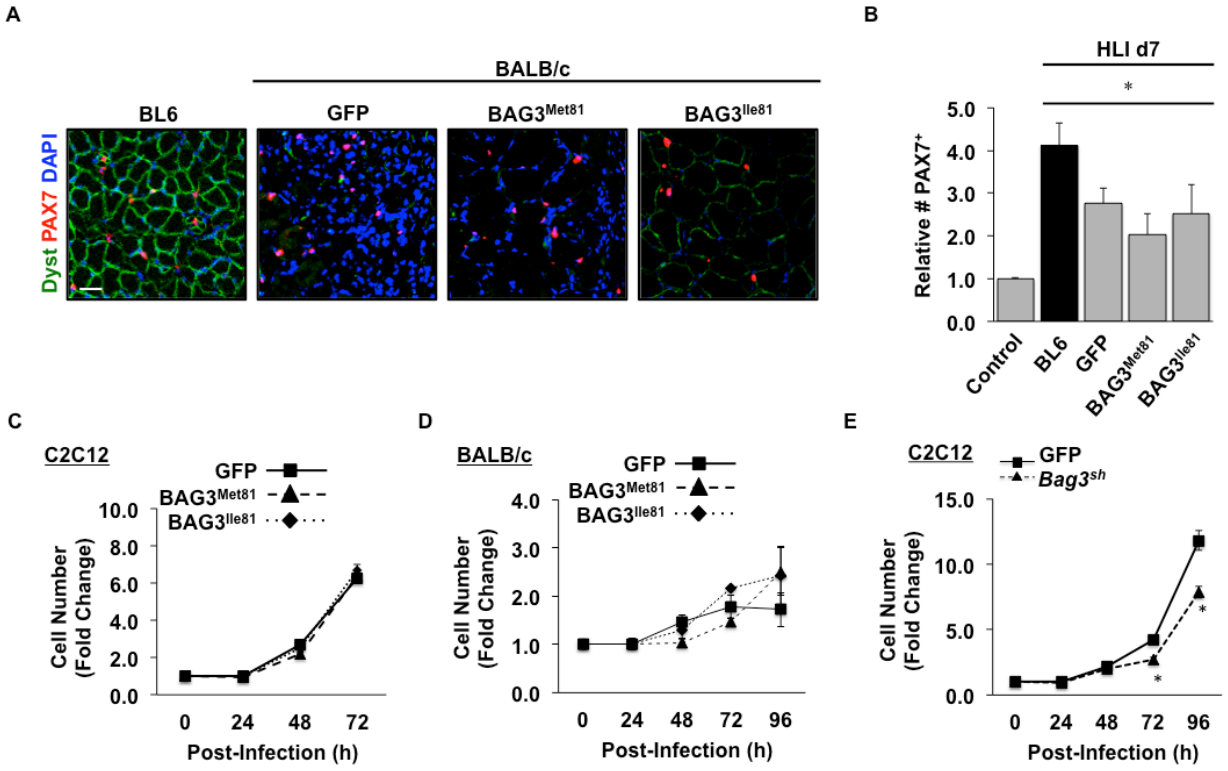

SFigure 7. BAG3 overexpression does not alter myoblast proliferation. A-B. BL6 and BALB/c mice were injected IM with the indicated AAVs then subjected to HLI for 7-days (N≥5 mice/group). TA muscle sections were stained with antibodies against the myogenic precursor cell marker PAX7 and dystrophin (Dyst, pseudocolored green) (**A**), and the density of $PAX7^{+}$ nuclei was quantified (**B**). * $P<0.05$ vs. Control. **C-D**. C2C12 myoblasts (**C**) or primary myoblasts isolated from BALB/c mice (**D**) were infected *in vitro* with Adenoviruses encoding GFP, $BAG3^{Met81}$, or $BAG3^{Ile81}$ and cell numbers were assessed at the indicated times as an indicator of proliferation (N ≥ 3). **E.** Viral knockdown of BAG3 ($Bag3^{sh}$, N ≥ 3) decreases cell number/proliferation in C2C12 cells *in vitro*. *$P<0.05$ vs. GFP control. All data are means ± SEM.

Supplemental Figure 8

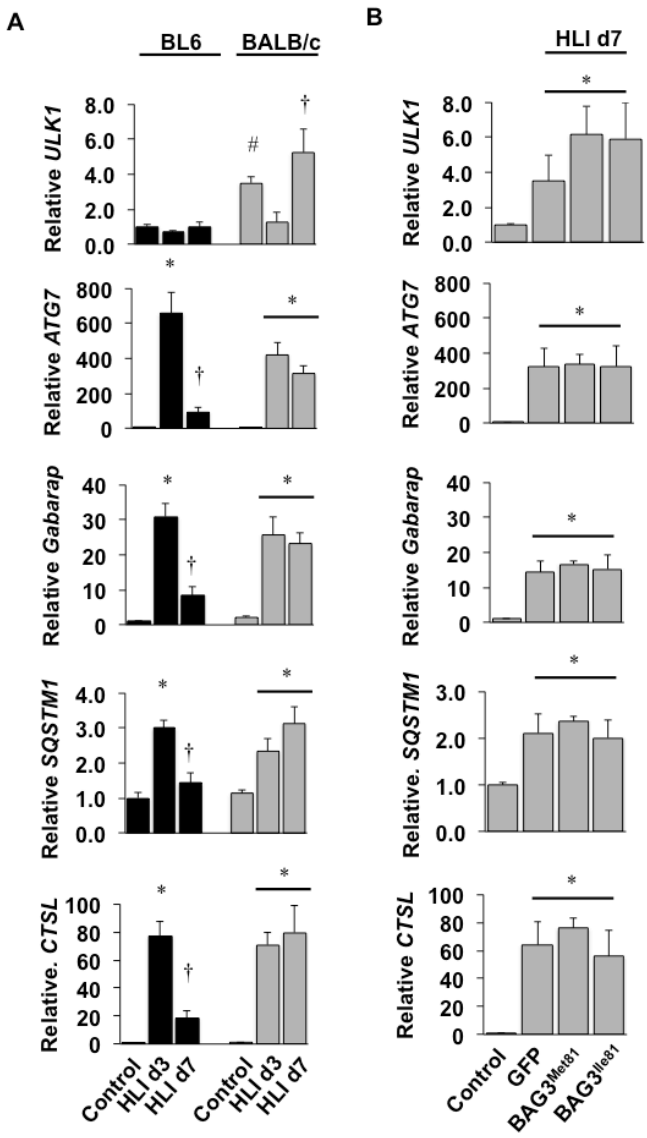

SFigure 8. Strain dependence of autophagy-related transcripts during limb ischemia. A. BL6 and BALB/c mice were subjected to HLI for 3 and 7 days, and RNA was isolated from limb muscle tissue for the quantification of the autophagy-related mRNAs ULK1, ATG7, Gabarap, SQSTM1, and CTSL by qRT-PCR, corrected for GAPDH, and normalized to expression in the contralateral control limb. *P<0.05 vs. strain-matched Control; †P<0.05 vs. strain-matched HLI d3. # P<0.05 vs. BL6 Control (*a priori* analysis). **B**. BALB/c mice (gray bars) injected IV with

AAVs encoding GFP (N=5), BAG3^{Met81} (N=10), or BAG3^{Ile81} (N=9) were subjected to modified HLI with collateral vessels left intact. RNA was isolated from limb muscle tissue for the quantification of autophagy-related mRNAs (ULK1, ATG7, Gabarap, SQSTM1, and CTSL) by qRT-PCR, corrected for GAPDH and normalized to expression in the contralateral control limb. **P*<0.05 vs. Control; †*P*<0.05 vs. HLI d7. All data are means ± SEM.

Supplemental Figure 9

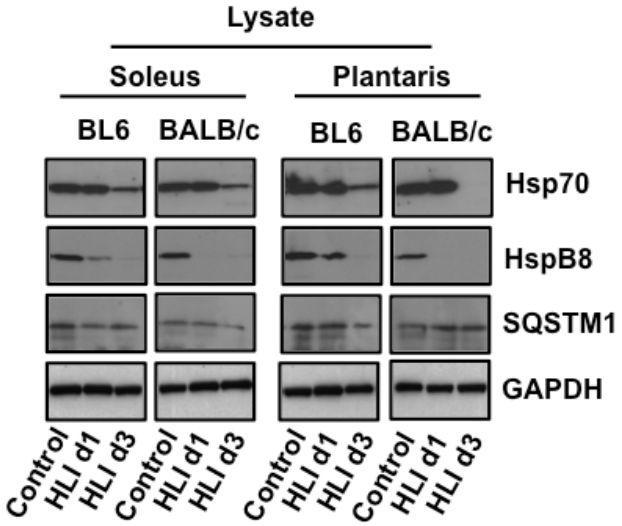

SFigure 9. Differential expression of BAG3 protein interactors during HLI in BL6 and BALB/c limb muscle. BL6 and BALB/c mice were subjected to HLI for 1 and 3 days, and protein was isolated from the soleus and plantaris limb muscles for western blotting. GAPDH was used as a loading control.

Supplemental Figure 10

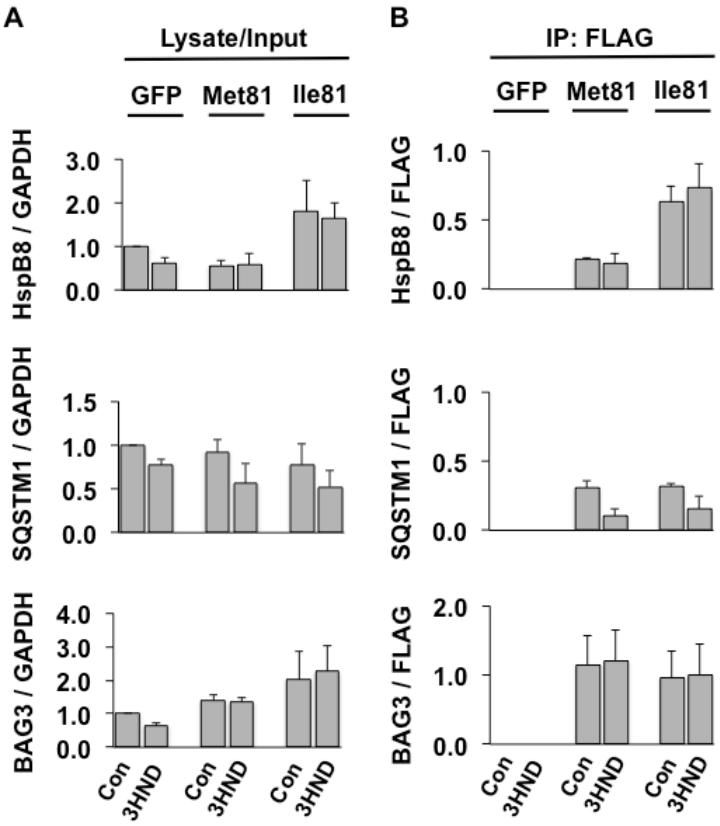

SFigure 10. BALB/c myotube protein abundances during ischemia. **A**. BALB/c primary muscle cells were infected with viruses encoding GFP, BAG3^{Met81}, or BAG3^{Ile81} and allowed to differentiate for 96h before experimental ischemia (3HND). Whole cell lysates were immunoblotted for HspB8, SQSTM1 (p62), and BAG3. Input/Lysate culture experiments were performed 3 independent times and protein abundances are graphically presented as corrected for GAPDH and normalized to GFP Control values for each independent experiment. **B**. FLAG-BAG3 was immunoprecipitated from input cell lysates (**A**) to examine the expression of BAG3 protein and the association of HspB8 and SQSTM1 with exogenously expressed BAG3. Immunoprecipitations were performed in 3 independent experiments and protein abundances are graphically presented as corrected for FLAG for each independent experiment.